Smart Design of Stable Extracellular Matrix Mimetic Hydrogel: Synthesis, Characterization, and In Vitro and In Vivo Evaluation for Tissue Engineering

*Oommen P. Oommen, Shujiang Wang, Marta Kisiel, Marije Sloff, Jöns Hilborn, and Oommen P. Varghese**

The simplicity and versatility of hydrazone crosslinking has made it a strategy of choice for the conjugation of bioactive molecules. However, the labile nature of hydrazone linkages and reversibility of this coupling reaction restricts its full potential. Based on the fundamental understanding of hydrazone stability, this problem is circumvented by resonance-stabilization of a developing N^2 positive charge in a hydrazone bond. A novel chemistry is presented to develop a resilient hydrazone bond that is stable and non-reversible under physiological conditions. A carbodihydrazide (CDH) type hydrazide derivative of the biomolecule forms intrinsically stabilized hydrazone-linkages that are nearly 15-fold more stable at pH 5 than conventional hydrazone. This chemoselective coupling reaction is catalyst-free, instantaneous, and virtually non-cleavable under physiological conditions, therefore can serve as a catalyst-free alternative to click chemistry. This novel crosslinking reaction is used to tailor a hyaluronan hydrogel, which delivered exceptional hydrolytic stability, mechanical properties, low swelling, and controlled enzymatic degradation. These desired characteristics are achieved without increasing the chemical crosslinking. The in vivo evaluation of this hydrogel revealed neo-bone with highly ordered collagen matrix mimicking natural bone regeneration. The proximity ligation assay or PLA is used to detect blood vessels, which highlighted the quality of engineered tissue.

1. Introduction

Polymer hydrogel network derived from synthetic macromolecules or biopolymers are extensively used for various biomedical applications.[1] These extensively hydrated networks are soft and elastic; often contain more than 90% water. Since they efficiently allow diffusion of small molecules, nutrients and oxygen, hydrogels provide an ideal 3D microenvironment for stem cell expansion and differentiation.[2,3] These materials are also used for various biomedical applications, such delivery of drugs[4] and proteins,[5] as bioadhesives,[6] as barriers for tissue or implants[7] and as scaffolds for regenerative medicine.[8] Among various hydrogel networks, hyaluronic acid (HA) or hyaluronan-derived hydrogel is extensively used for medical applications, such as viscosupplement for osteoarthritis treatment,[9] ocular surgery,[10,11] skin fillers,[12] drug delivery,[13] and tissue regeneration.[14,15] Native HA also plays a pivotal role in vivo for cell and tissue integrity, cell proliferation, wound repair, inflammation, morphogenesis and intracellular signaling.[16] We have recently shown that HA hydrogel can be used as an injectable carrier for bone morphogenetic protein-2 (BMP-2) for in vivo bone tissue engineering.[17] An important criterion for any hydrogel design is the control over swelling of these materials when used in vivo as implants or devices. However, excessive and uncontrolled swelling is generally encountered in hydrogel systems in vivo, which significantly hampers its performance. This results in poor tissue regeneration,[18] affecting stem cell differentiation,[19] and triggering burst release of drugs or proteins.[20] This biomaterial engineering challenge is currently circumvented by extensive crosslinking, which increase gel rigidity and retards degradation.[21,22] Such crosslinking requires extensive chemical modification of the native macromolecules, which adversely affects its biological recognition, which in turn compromises cell viability and spatial organization of encapsulated cells[23] limiting efficient tissue regeneration.[24]

In our effort to develop stable yet native ECM mimetic hydrogel system for clinical application, we present a novel approach for designing hydrogel with tunable swelling properties without increasing chemical crosslinking. The swelling of hydrogel, in general, may be described by the Flory and Rehner theory, which states that when a polymeric network is

Dr. O. P. Oommen, S. Wang, Dr. M. Kisiel, Prof. J. Hilborn, Prof. O. P. Varghese
Department of Chemistry, SciLifeLab Uppsala
Ångström Laboratory, Uppsala University
75121 Uppsala, Sweden
E-mail: oommen.varghese@kemi.uu.se
M. Sloff
Urology – Experimental Urology 267
Nijmegen Medical Centre
Radboud University
6525 GA Nijmegen, The Netherlands

DOI: 10.1002/adfm.201201698

immersed in a suitable solvent to attain thermodynamic equilibrium the network chains experiences two opposing forces, the thermodynamic force of mixing and retractive force of the polymer chains.[1] Several factors contribute to control the swelling extent and eventual disintegration. Key factors that regulate these processes are polymer-solvent interaction, molecular weight of precursor polymer, number and length of crosslinks, and stability of the crosslinks.[1,18]

We decided to investigate this phenomenon utilizing dynamic covalent chemistry of hydrazones with different crosslinkers having unique properties. The advantage of using this chemistry is that it offers good temporal control over the reaction with almost quantitative coupling within seconds, without need for any catalysts or initiators. This method also minimizes intramolecular crosslinking (loop formation) as the two orthogonal functional groups are placed on two complementary polymers. The drawback of this type of linkage however, lies in the poor stability of this derivative under physiological conditions.[25]

In our pursuit to develop stable hydrazone linkage, we discovered a new hydrazone system, which is intrinsically stabilized by delocalization of positive charge. This proficient coupling strategy offers new avenues to develop robust materials with tunable hydrolysis and swelling characteristics. Utilizing this chemistry, we engineered HA based injectable hydrogels that showed exceptional stability with controlled swelling and enzymatic degradation. In vitro and in vivo evaluation of this material showed that such modifications are well tolerated by cells and can be used for in vivo delivery of growth factor for bone tissue regeneration.

2. Results

2.1. Discerning Hydrazone Stability by Fine-Tuning Electronic Character

Hydrolytic stability of hydrazone linkage is crucial for developing hydrazone coupled biomolecules. The fundamental hydrolysis mechanism of hydrazone, oxime or imine, involves the protonation of N^1 followed by nucleophilic attack of water (**II**, **Figure 1**).[26] However, in hydrazones and oximes the neighboring heteroatom (X) gets protonated first **VI**, (due to significantly higher pKa of X as compared to N^1) making it less susceptible towards nucleophilic attack by water.[26] Thus, the key for designing molecules with resilient hydrazone bond, the molecule should possess ability to prevent protonation of N^1, which could be achieved either by using aromatic aldehyde substrate for developing hydrazone[27] or by increasing the electron density of N^2. As using aromatic aldehydes limits the scope and versatility of this coupling, we envision that this could also be achieved by stabilization of developing positive charge on N^2. Thus we attempted to fine-tune the electronic character of the R_1 moiety, to modulate the extent of protonation of X group (Figure 1).

We therefore synthesized three different hydrazide functionalized HA derivatives that has unique electronic character. The dihydrazides namely, carbodihydrazide (CDH), oxalyldihydrazide (ODH) and adipoyldihydrazide (ADH) derivatives of HA were prepared employing standard carbodiimide coupling in presence of *N*-hydroxybenzotriazole (HOBt) with 10 fold excess of dihydrazides (with respect to the carbodiimide) to promote monosubstitution (Figure S1 in the Supporting Information).[28] We optimized this coupling chemistry by tuning the reaction pH to obtain 7 to 8% hydrazide modifications of HA (Table S1 in the Supporting Information). These HA derivatives were purified by dialysis to obtain the desired products in pure form as determined by ^{1}H NMR. The degree of hydrazide modifications was determined following literature procedure using trinitrobenzene sulfonic acid (TNBS) assay, which gives a quantitative assessment of free hydrazide residues using UV spectroscopy.[28] To investigate the hydrolytic stability of these three HA hydrazide derivatives we synthesized model HA hydrazones with 4-hydroxybenzaldehyde (termed as CDH-hydrazone, ODH-hydrazone and ADH-hydrazone) and evaluated their hydrolytic stability at pH 5.0. Hydrolysis rate was determined by performing dialysis of HA hydrazones at this pH and the amount of 4-hydroxybenzaldehyde released was evaluated by measuring the UV absorbance of release medium at different time points at 285 nm. Interestingly, we observed significant differences in the hydrolytic behavior of these hydrazones (**Figure 2**a). While ODH-hydrazone and ADH-hydrazone released 50% of 4-hydroxybenzaldehyde within 20 h (at 8 and 19 h, respectively), the CDH-hydrazone on the other hand, showed much slower release profile with 50% release at 305 h (Figure 2a). The reaction did not, however, follow strict pseudo-first order kinetics, as we did not observe good curve fitting to determine the half-life accurately.

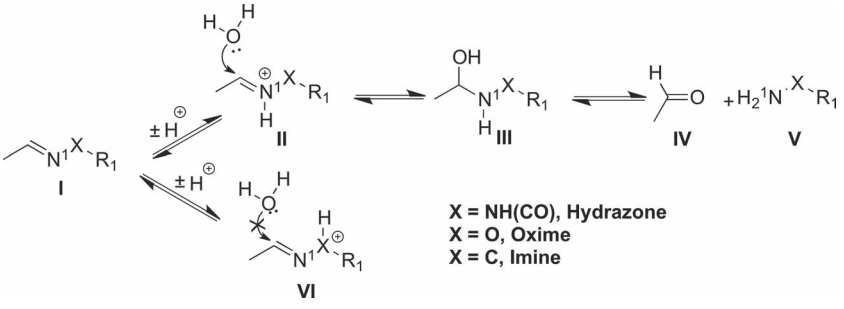

Figure 1. Putative mechanism of hydrolysis of hydrazone, oxime, and imine.

2.2. HA-Hydrogel Synthesis and Characterization

To examine how hydrolytic stability of the hydrazone crosslinks translates into degradation and swelling characteristics of a hydrogel system, we developed hydrazone crosslinked hydrogel with 150 kDa HA aldehyde and three 150 kDa HA hydrazides which we termed as CDH-gel, ODH-gel and ADH-gel (Figure 2c). HA aldehyde was synthesized following our previously described protocol with 7% modification.[17] This method is superior to conventional methods of $NaIO_4$ oxidation as the aldehyde units were grafted as pendent group on HA under mild conditions without any oxidation of cyclic sugar residues. Hydrogels were prepared

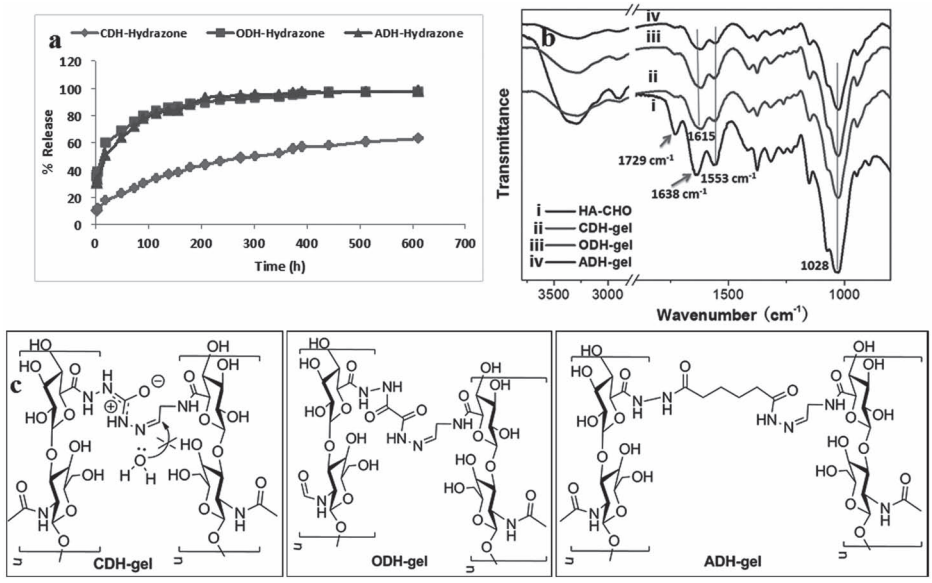

Figure 2. Hydrazone stability, structure and characterization. a) Hydrolytic stability of 4-hydroxybenzaldehyde hydrazone as determined by UV spectroscopy. b) ATR-FTIR spectrum of HA modified with aldehyde (in black) and corresponding lyophilized hydrogels. This spectrum indicates disappearance of the aldehyde signal at 1729 cm^{-1} in all the three gels indicating complete crosslinking by hydrazide functionality. Moreover, the amide-I signal at 1638 cm^{-1} overlaps with the hydrazone (C=N stretching) signal resulting a shift to 1615 cm^{-1}. The carboxylate (C=O) signal and alcohol (C-O) appeared at 1553 cm^{-1} and 1028 cm^{-1} respectively in all the four samples. c) Representative chemical structure of the three type of hydrazone crosslinked HA hydrogel.

by mixing a 1:1 weight ratio of the two HA-derivatives (aldehyde and hydrazide) with total solid content of 16 mg in 1 mL (1.6 wt%). The conversion of the crosslinking reaction was determined by infrared (IR) spectroscopic analysis of lyophilized hydrogels. The IR spectrum of lyophilized gel samples showed that the aldehyde peak at 1729 cm^{-1} completely disappeared in all the three gel samples, indicative of complete conversion of the reactions (Figure 2b). The appearance of a peak at 1615 cm^{-1} is attributed to the formation of the desired hydrazone with its characteristic C=N stretching (Figure 2b).

2.3. Rheological Studies

Rheological characterization of these hydrogels was performed at frequency sweep from 0.1–10 Hz on these hydrogels (**Figure 3**a). **Table 1** shows the gel characteristics of these materials after 24 h. The loss tangent (tan δ), that gives a measure of energy loss in the material upon deformation, was shown to be <1 in all cases.[29] This demonstrates predominantly elastic rather than viscous behavior of the hydrogels (Table 1) which is typical for ideal gels with few loops, dangling ends or physical entanglements. To understand the structure-property relationship as a result of hydrogel crosslinking chemistry, we examined the storage modulus of the gels to extract information on the average mesh size (ξ) as well as the average molecular weight between crosslinks (Mc) in the hydrogel.[22,30,31]

The average mesh size (distance between two crosslinks or entanglement points) ξ was calculated based on rubber elastic theory that can be applied on hydrogels that has elastic character.[31] The Mc and ξ parameters were derived from the following Equations 1 and 2:

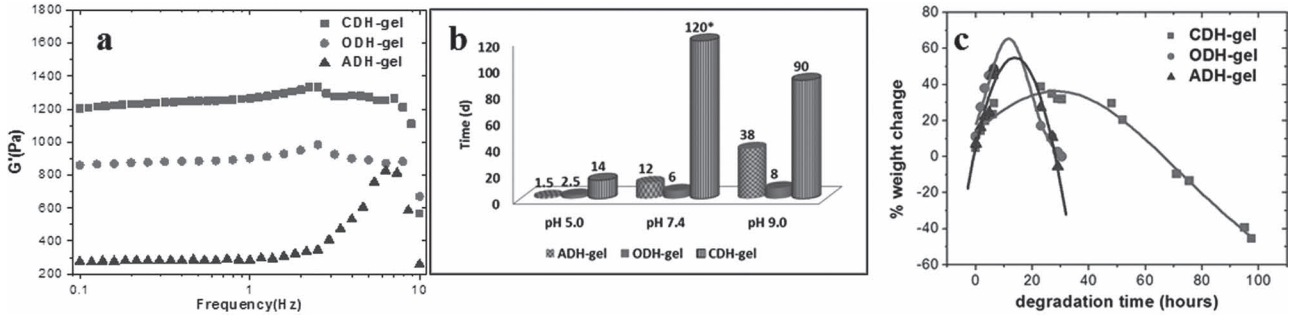

Figure 3. Hydrogel swelling and characterization. a) Storage modulus G' as a function of frequency. b) Degradation study of hydrogels at different pH. The * indicates no change in morphology and no disintegration observed throughout the study. c) Degradation of gel in presence of hyaluronidase enzyme in 7.4 pH phosphate buffered saline (PBS).

Table 1. Rheological data of HA-hydrogels.

HA-gel[a)]	%[b)]	G' [Pa]	G'' [Pa]	tan δ[c)]	Mc [kg/mol]	ξ [nm]
CDH-gel	7	1196 ± 65	3.1 ± 0.3	0.0026	33	15.1
ODH-gel	8.2	956 ± 67	8 ± 0.84	0.0083	41	16.2
ADH-gel	7.4	297 ± 25	5.4 ± 0.84	0.018	129	23.9

[a)]Hydrogels made in PBS 7.4 and measured after 24 h; [b)]degree of modification on HA backbone; [c)]tan $\delta = G''/G'$; ξ = average mesh size.

$$Mc = \frac{c\rho RT}{G'p} \quad (1)$$

$$\xi = \left(\frac{G'N_A}{RT}\right) \quad (2)$$

where c is the polymer concentration (1.6% w/v), ρ is the density of water at 298 K (997 kg m^{-3}), R is molar gas constant, $G'p$ is the peak value of G' (Figure S2, Supporting Information), N_A is the Avogadro constant and T is temperature (298 K).

2.4. Hydrogel Swelling and Stability Studies

We subsequently investigated the hydrolytic stability of the gels by performing swelling/disintegration studies of these gels and estimated the% weight change using Equation 3:

$$\%\ \text{weight change} = \frac{w_1 - w_0}{w_0} \times 100 \quad (3)$$

where, w_0 is the weight of gel before swelling and w_1 is the weight of gel after swelling. The swelling experiments were carried out under acidic (5.0 pH acetate buffer), basic (9.0 pH PBS buffer) and neutral (7.4 pH PBS buffer) conditions.

Degradation studies (in days) of the gels revealed that the CDH-gel was significantly more stable in all tested conditions as compared to the ODH and ADH gels (Figure 3b). It is remarkable to note that under acidic condition (5.0 pH), where hydrazone linkage generally are unstable, the CDH-gel survived for 14 days while at pH 9.0 it slowly disintegrated in 90 days (Figure 3b). Interestingly, at physiological pH the CDH-gel retained its morphology even after 4 months with slow swelling. Encouraged by these results we examined the stability of the gel in presence of hyaluronidase, the enzyme known to degrade HA in vivo. Remarkably, in presence of hyaluronidase both ODH-gel and ADH-gel completely disintegrated within 40 h, while the CDH-gel disintegrated slowly in about 100 h (Figure 3c).

2.5. In Vitro Evaluation

Next, we evaluated if such chemical modifications of HA does have any adverse effects on cells. For this we performed MTS assay, which measures the mitochondrial activity of live cells, indirectly indicating cell viability. We performed this assay with all HA components as well as with hyaluronidase degraded gels. As shown in Figure S3 in the Supporting Information, none of the HA products showed any toxicity at low (100 µg/µL) or high (200 µg/µL) concentrations. On the contrary, the HA components in fact increase fibroblast proliferation as compared to the control, which is a known phenomenon caused by HA interaction with cell-surface receptors.[32]

2.6. In Vivo Evaluation of Ectopic Bone Formation

Finally, we examined the efficacy of our best hydrogel (CDH-gel) to deliver a therapeutic protein namely, recombinant human BMP-2 (rhBMP-2) in a rat subcutaneous model for bone regeneration. Histological evaluation with H&E and Masson's trichrome of the bone tissue harvested after 7 weeks of post-implantation revealed that the neo-bone have trabecular structure with bone marrow as in mature bone. The representative cross sections stained with H&E and Masson's trichrome as shown in **Figure 4**a,b, revealed a well-mineralized tissue with abundant adipocytes (large white colonies)[33] and no inflammatory cells. In order to determine the quality of neo-bone we investigated collagen-orientation and blood vessel formation in this tissue. We anticipated that slower degradation and controlled swelling of CDH-gel will facilitate recruited stem cells that differentiate, to lay-down matrix in a controlled fashion as in natural bone. Thus we performed picrosirius red staining, which allow visual quantification of natural birefringence of oriented collagen as green stain while disoriented collagen, appears as red under polarized light microscope (Figure 4c). The organized collagen matrix observed in our new bone signifies the potential of our material for bone regeneration.

Angiogenesis (blood vessel formation) within the neo-bone tissue is a significant parameter for healthy bone tissue

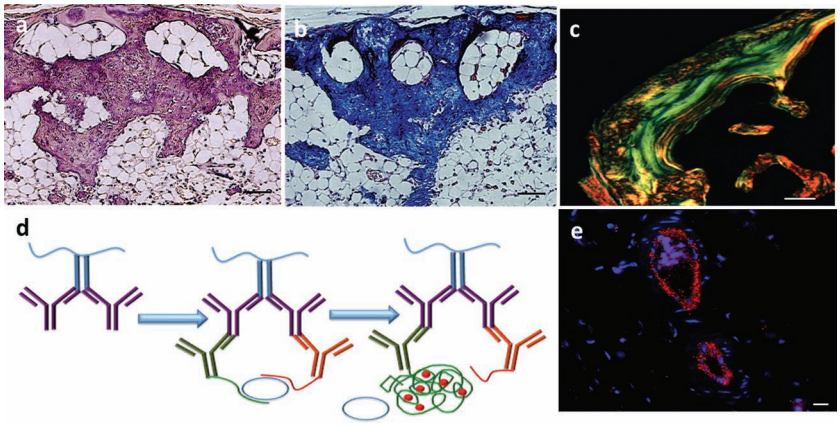

Figure 4. Histological examination of ectopic bone harvested after 7 weeks post implantation. The representative cross-sections were stained with a) hematoxilin/eosin (H&E); b) Masson's trichome; and c) picrosirius red. d) Schematic outline of the in situ PLA strategy showing: i) detecting RECA-1 primary antibodies; ii) close proximity of oligonucleotide-ligated secondary antibodies allows a rolling-circle amplification (RCA); and iii) detection of the RCA product by a fluorescently labeled probe. e) In situ PLA detection of anti-RECA-1 in histological samples. Scale bars are: (a,b) 100 µm, (c) 500 µm, and (e) 10 µm.

regeneration, which is difficult to evaluate using conventional immunohistochemical analysis. Here we employed a new technique in our histological samples called proximity-ligation assay (PLA), which intensifies the protein detection process through an indirect signal amplification process (Figure 4d).[34,35] In this technique individual or complexes of protein are first detected using primary antibody, similar to conventional immunodetection assay. This is followed by addition of modified secondary antibody with attached oligonucleotide (step ii, Figure 4d). The specific sequence of oligonucleotide is detected by bridging probe that bind oligonucleotide in a proximity dependent manner, which upon ligation, allows rolling-circle amplification. This amplified DNA strand is finally stained with DNA detecting fluorescent dye, which consequently enhances specificity and sensitivity of the protein of interest (step iii, Figure 4d). By exploiting this technique in our histological samples, we for the first time visualized blood vessels in the ectopic bone by targeting rat specific endothelial marker anti-RECA-1 within the tissue (Figure 4e).

3. Discussion

Dynamic covalent coupling of hydrazone has been extensively exploited for bioconjugation since this bond is relatively stable at physiological pH while cleavable at acidic pH. However, it cannot be used as an alternative to click reactions as these bonds undergo slow hydrolysis at physiological pH.[25] Here we present a novel strategy to circumvent this limitation by designing intrinsically stabilized hydrazone bond. This was achieved by devising a hydrazone linker possessing a neighboring heteroatom (N^3), which provides resonance stabilization to the developing N^2 positive charge, analogues to the classical α-effect stabilization.[36] Specifically, we demonstrate that hydrazone derived from CDH ($C^1{=}N^1{-}N^2H{-}(C{=}O)N^3H$) type linker allows delocalization of N^2 positive charge due to its urea-type structure (Figure 2c). For comparison ODH and ADH counterpart were evaluated where such stabilization is absent. The ODH-hydrazone, on the other hand, may have stabilization due to the negative inductive effect of the additional carbonyl group, which could prevent protonation of N^1 and N^2 (Figure 2c). The resonating structures of these three types of hydrazones are represented in **Figure 5**, which clearly illustrates extensive resonance stabilization in CDH-hydrazone, unlike ODH and ADH analogs.

Our hypothesis was verified by determining the rate of hydrolysis of hydrazone bonds obtained from HA hydrazide derivatives and 4-hydroxybenzaldehyde. It is noteworthy that under acidic condition (pH 5.0) where hydrazones are generally unstable, nearly 15-fold increase in stability of CDH derived hydrazone was observed as compared to other hydrazones (Figure 2a). Interestingly, at physiological pH we did not observe any release of 4-hydroxybenzaldehyde (data not shown). Our result clearly demonstrates that CDH-hydrazone forms non-reversible and stable chemical linkages at physiological pH offering an exciting catalyst free alternative for click reaction.

The improved hydrolytic stability encouraged us to develop HA-hydrogels with these three types of hydrazide derivatives. We intentionally maintained a very low degree of modification (7–8%) of each reactive functional group, as the focus

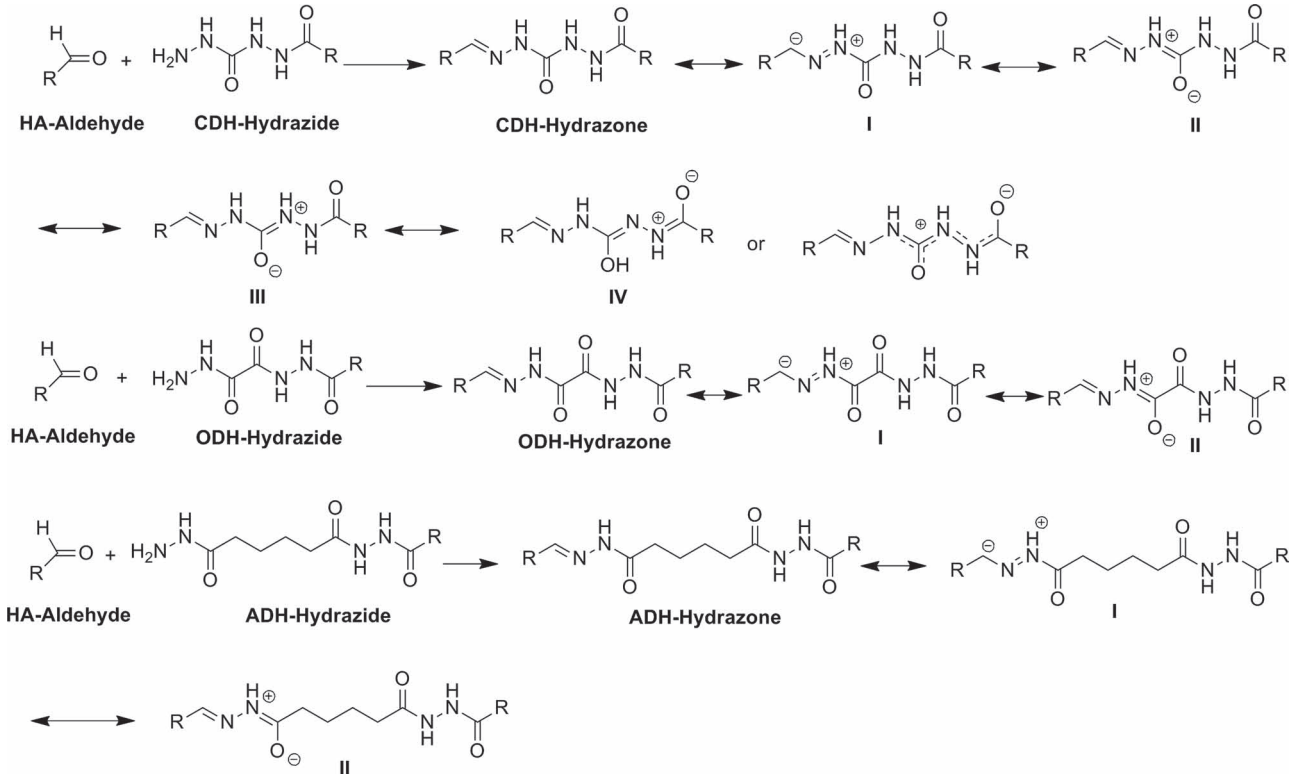

Figure 5. Major resonance structure of different HA hydrazones.

of our work was to develop robust hydrogel with minimum modification of the ECM component. Hydrogels were obtained within 30 s upon mixing 1:1 weight ratio of HA-aldehyde and HA-hydrazide derivatives. Efficient hydrazone formation was observed in all cases as determined by IR spectra of lyophilized gels (Figure 2b). The rheological experiments of these hydrogels confirmed that although HA-CDH modification had slightly lower hydrazide residues (7%) as compared to ODH (8.2%) and ADH (7.4%) derivatives, it resulted in formation of more mechanically robust gel with higher crosslinking density as shown by the lower *Mc* and ξ (Table 1). The ADH gel on the other hand had ξ as high as 23.9 nm, possibly due to its more hydrophobic linker. We further investigated the stability of these gels in acidic, basic and physiological conditions, which clearly corroborated with the kinetic studies of hydrazones. Although CDH-gel and ODH-gel had nearly the same average mesh size (ξ, 15–16 nm) as well as the average molecular weight between crosslinks (*Mc*, 33 and 41 kg/mol respectively), they demonstrated striking difference in their swelling and degradation behavior. It is exciting to note that under physiological conditions, the CDH-gel retained its morphology even after 4 months. Interestingly, the increased stability of the crosslinks was also reflected in hyaluronidase mediated enzymatic degradation of hydrogel. Such differences in enzymatic degradation profile of hydrogels are generally observed by increasing the crosslinking density of the material.[37] This controlled enzymatic degradation and swelling of gels without compromising the biological function (by minimum chemical modification of native HA structure) is a significant accomplishment for biomaterial applications. Such materials with controlled swelling and employing mild crosslinking conditions could be used as drug depot for drug delivery, 3D cell culture matrix, expansion of embryonic stem cells and for encapsulating therapeutic proteins and growth factors.[2,3] We also performed in vitro cytotoxicity (MTS) assay with the hydrogel components as well as enzymatic degradation products since such soluble and degradation products are responsible for in vivo toxicity. These experiments confirmed that such chemical modifications and hydrogel degradation products are well tolerated by cells.

Finally we tested the efficiency of our new material as an rhBMP-2 carrier in vivo, in a rat subcutaneous model. Though the therapeutic potential of BMP-2 is well established, finding effective methods to deliver clinically effective dose of BMP-2 is still an unmet challenge. It is known that high dose to this protein has adverse side effects,[38] whereas, low dose is ineffective. Thus an optimum delivery system is required that can efficiently regenerate tissue with lower dose of the growth factor. For preliminary screening of our material in vivo, we tested CDH hydrogel with a very low dose of rhBMP-2 (InductOs) that is approved by Food and Drug Administration (FDA) for specific clinical application. Due to controlled swelling behavior of our hydrogel we tested significantly lower dose of BMP-2 (20 μg/mL or 4 μg per implant), as compared to our previous studies (150 μg/mL BMP-2 or 30 μg per implant).[17] Bone regeneration with lower therapeutic dose will have major implications in clinical use of rhBMP-2. Histological analysis of ectopic bone showed surprisingly well-mineralized bone with abundant adipose tissue. This characteristic is generally observed at a very high dose of BMP-2 (600 μg/mL) where stem cell commitment towards adipogenesis is turned-on over osteogenesis.[33] This effect is due to activation of the transcription factor peroxisome proliferator activated receptor gamma (PPARγ), a key regulator of adipogenesis.[39]

Another remarkable finding in this experiment was the observation of oriented collagen matrix at the periphery of the tissue, which is relatively rare especially at a site where natural bone does not exist (ectopic site). The anisotropic nature of oriented collagen could be detected as green using polarized light microscope after picrosirius staining. Improved characteristics of this scaffold could be responsible for such observation since fast degradable gels has lower impact on cell recruitment and osteoblast mediated organized matrix formation.[40,41] Oriented collagen also implies that the lamellar structure of the engineered bone possess close parity with natural bone remodeling and can possess load bearing capability.[41] To demonstrate blood vessel formation within the newly formed tissue, we employed an advanced technology of PLA. This is the first report of detecting rat vascular endothelium using anti-RECA-1 and amplifying protein signal using PLA technique.

4. Conclusions

In summary, we have demonstrated that fine-tuning of the charge distribution over the hydrazone moiety could provide intrinsically stabilized hydrazone bonds making it resilient to hydrolysis. We found that grafting CDH hydrazide on biomolecules can deliver an exceedingly stable hydrazone linkage, which is nearly 15 fold more stable (at pH 5.0) than other hydrazones. This coupling chemistry is catalyst-free, chemoselective, instantaneous and non-reversible under physiological conditions. We utilized this coupling strategy to develop HA based ECM mimetic hydrogel. This hydrogel demonstrated astounding stability at acidic, basic and physiological pH. The stability of such linkages was also reflected in the mechanical properties of the material, which resulted in controlled swelling and enzymatic degradation characteristics. Our preliminary in vivo evaluation of this hydrogel as an rhBMP-2 carrier showed mature bone formation with oriented collagen and angiogenesis with several folds lower dose of growth factor. The injectability of such materials is equally important for clinical applications, as it is amenable to minimal invasive procedures. The low cost for manufacturing, easy scalability, non-toxicity, and established biocompatibility of HA based materials will favor translation of such materials for clinical application.

5. Experimental Section

Materials and Methods: Hyaluronic acids (HA, 150 kDa) were purchased from Javenech SA, HTL SAS (Javene-France). All other reagents were purchased from Sigma-Aldrich (Sweden) and used as received. All solvents were of analytical quality (p.a.) and were dried over 4 Å molecular sieves. Dialysis membranes were purchased from Spectra Por-6 (MWCO 3500). The NMR experiments (δ scale; J values are in Hz) were carried out on Jeol JNM-ECP Series FT NMR system at a magnetic field strength of 9.4 T, operating at 400 MHz for ^{1}H. AR2000 Advanced Rheometer (TA Instruments) was used for rheology measurement.

Spectrum One AT-FTIR and Lambda 35 UV-Vis spectrophotometer from PerkinElmer instruments were used for spectroscopic analysis.

Synthesis of HA-Aldehyde Derivative: Synthesis of aldehyde derivative of HA was done following a previously reported procedure.[17]

Synthesis of Hydrazide Derivative of HA: HA (408 mg, 1 mmol of disaccharide repeat units) was dissolved in 100 mL de-ionized water at room temperature, dihydrazide (1 mmol, CDH or ADH) was added followed by HOBt (153 mg, 1 mmol). Thereafter, pH of the resultant solution was adjusted as shown in Table S1 (Supporting Information) and solid EDC (1-ethyl-3-(3-dimethylaminopropyl) carbodiimide; 19.17 mg, 0.1 mmol) was added and stirred overnight. The solution was loaded into a dialysis bag (Spectra Por-6, MWCO 3500) and dialyzed against dilute HCl (pH = 3.5) containing 0.1 M NaCl (2 × 2 L, 48 h), then dialyzed against deionized water (2 × 2 L, 24 h). The solution was lyophilized and 360–390 mg HA-hydrazide derivative (7–8% modification) was obtained.

A modified procedure was adopted to synthesize HA-ODH as only 2.6% coupling was obtained at pH 4.7. The reaction was optimized at different pH and best coupling of 4.1% was observed at pH 4.0 (see Table S1, Supporting Information). In order to secure 7–8% modifications, double amount of EDC (38.3 mg, 0.2 mmol) was used. The ^{1}H NMR analysis did not show any difference for HA-ODH and HA-CDH derivatives as compared to the native HA, however the HA-ADH spectra was identical with our previously published article.[28]

Synthesis and Kinetic Study of HA-Hydrazone with 4-Hydroxybenzaldehyde: For performing kinetic study, HA hydrazide derivatives with CDH, ODH and ADH were synthesized with 14–15% modification by doubling the amount of EDC reported earlier. The degree of free hydrazide moiety was estimated by TNBS assay. HA hydrazone was subsequently synthesized from 4-hydroxybenzaldehyde and HA- hydrazides. Briefly, HA-hydrazide (20 mg, 0.05 mmol of disaccharide repeat units) was dissolved in 1 mL of PBS 7.4 (pH of the reaction mixture was found to be around 5.5-5.8). Excess of 4-hydroxybenzaldehyde (7.32 mg, 0.06 mmol) dissolved in 0.2 mL PBS was added and stirred for 4 h. The reaction mixture was transferred to Slide-A-Lyzer MINI Dialysis Device, 3.5 K MWCO, 2 mL fitted on a glass chamber containing 18 mL of PBS 7.4. The sample was placed on a shaker (150 rmp) for 24 h, and amount of 4-hydroxybenzaldehyde released to the medium was calculated by UV measurement at 285 nm. The buffer in the release medium was replaced with fresh PBS buffer and dialysis was continued for another 6 h till no further increment in UV absorbance was observed. The amount of 4-hydroxybenzaldehyde used for hydrazone was quantified (deducted from the cumulative absorbance of release medium) to be around 14%, which corroborated with hydrazide modification. Thereafter, the dialysis bag was suspended in 18 mL fresh acetate buffer (pH 5.0), and placed on the shaker (150 rpm) and UV absorbance of the release medium was measured at different time points.

Preparation of HA Hydrogels: HA-aldehyde derivative (4 mg, 7% modification) was dissolved in sterile PBS (250 µL, pH 7.4) at a concentration of 16 mg/mL and filtered through sterile 0.45 µm syringe filter (Pall Corp., East Hills, NY). HA-hydrazide derivative (4 mg, 7–8% modification) was also dissolved in sterile PBS (250 µL, pH 7.4) to get the same concentration (16 mg/mL) and filtered through sterile 0.8 µm syringe filter (Pall Corp.). Materials were loaded into two 1 mL luer-lock syringes with a volume ratio of 1:1. The two syringes were connected at the tip with luer-lock adapter and the two solutions were mixed for 20 cycles at room temperature. The duration of mixing process was around 30 s. All solution passing through one syringe to the other was considered as one mixing cycle. The mixture was injected to cylinder mold immediately after mixing. Molds were carefully covered with Parafilm M and kept for 24 h at room temperature to obtain complete crosslinking.

Hydrogel Stability Study: Hydrogels from HA-aldehyde and different HA-hydrazides were prepared in 500 µL at a concentration of 16 mg/mL as described earlier. After 24 h at room temperature the gels were removed from the mold and were suspended in different 6 mL mediums (5.0 pH acetate buffer, 7.4 pH PBS buffer, 9.0 pH PBS buffer). Medium was removed at different time points and weights of the gel were measured and were replenished with fresh medium till the gels disappeared. For the enzymatic degradation experiment, 500 µL of respective gel was suspended in 3 mL PBS 7.4 pH containing 25 U hyaluronidase/mL. After removing the supernatant, the weight of the gels were measured at different time points and replenished by fresh medium containing the enzyme. Weight loss was calculated using Equation 3.

Rheological Evaluation: An AR2000 Advanced Rheometer (TA Instruments) was used to determine the rheological behavior. The gel was prepared in mold as described above and carefully transferred to the AR2000 Advanced Rheometer. The rheological properties were determined with frequency from 1–10 Hz at 25 °C using 8 mm aluminum plate geometry. The gap was adjusted starting from the original sample height and compressing the sample to reach a normal force of about 30 mN (gap sizes were between 2 and 3 mm). From the minimum of tan δ, in linear viscoelastic region, $G'p$ can be obtained from G'-frequency curve. $G'p$ of CDH-gel, ODH-gel and ADH-gel were 1206, 943 and 305 Pa respectively.

In Vitro Cell Culture and Cytotoxicity Assay: Mouse embryonic fibroblast cells, NIH 3T3 (American Type Culture Collection (ATCC)-LGC standards, Sweden) were cultured in Dulbecco's Modified Eagle Medium (DMEM) and F-12 Ham (1:1) (Sigma-Aldrich), supplemented with 10% fetal bovine serum (FBS Hyclone, Perbio Scientific, Sweden) and 1% antibiotics (10 000 U penicillin and 10 mg/mL streptomycin, Sigma-Aldrich).

One day prior to the assay, NIH 3T3 cells were seeded in 96-well plates at a density of 5.0×10^3 cells per well in 100 µL medium. After an overnight incubation, the medium was removed and replaced with fresh medium, containing 100 µg/mL or 200 µg/mL HA derivatives or hyaluronidase (10 Units/mL) mediated gel degradation products that were heat inactivated for 20 min at 100 °C ($n = 3$). Cell viability in response to the biomaterials was measured using an MTS [3-(4,5-dimethylthiazol-2-yl)-5-(3-carboxymethoxyphenyl)-2-(4-sulfophenyl)2H tetrazolium] cytotoxicity assay (CellTiter 96 AQueous Non-Radioactive Cell Proliferation Assay, Promega), according to the manufacturer's instructions.

Briefly, after 48 h incubation with respective biomaterials, 20 µL of substrate was directly added to the incubation medium and cells were maintained for an additional 4 h in a humidified incubator at 37 °C and 5% CO_2. The absorbance at 450 nm was determined using Labsystems Multiskan MS plate reader (Labsystems).

Reconstitution of rhBMP-2: RhBMP-2 (Pfizer, InductOs former Wyeth Europe Ltd., Berkshire, UK) was reconstituted according to the manufacturers protocols. The stock solution of BMP-2 was prepared at a concentration of 1.5 mg/mL and stored at 4 °C.

Hydrogel Preparation for In Vivo Application: Each of the HA hydrazide and HA aldehyde derivatives were dissolved separately in PBS, at pH 7.4 to obtain a final concentration of 16 mg/mL, which was sterile filtered using 0.45 µm syringe filter (Whatman). The reconstituted stock solution of rhBMP-2 was added to the HA-hydrazide solution to maintain final concentration of 16 mg/mL of polymer and 20 µg/mL of protein. HA hydrogel matrix was formed by mixing equal volume of HA-aldehyde and HA-hydrazide solutions in two syringes linked by a connector under sterile conditions in a laminar flow hood.

In Vivo Rat Model: Animal Preparation: All animal handling and surgical procedure were approved by the Uppsala (Sweden) local committee for experimental animal research ethics (246/8) and conducted according to the Helsinki guideline for the use and care of laboratory animals. Six adult male Sprague-Dawley rats (Taconic M&B, Lille Skensved, Denmark), 280–300 g in weight were housed with two rats per cage with 12/12 h light/dark cycles in a temperature (22 °C) and humidity (45% ± 10%) controlled environment with ad libitum access to food and water. All surgical procedures were performed in aseptic conditions. Animals were anesthetized by using Isoflurane (4,5% induce; 2.5% maintain; Forene, Abbott Scandinavia, Solna, Sweden) starting with 4 L min^{-1} oxygen and 4 L min^{-1} isoflurane in an induction chamber and then by mask at 1.5 L min^{-1} oxygen, 1.5 L min^{-1} air and 3 min^{-1} isoflurane.

Surgical Technique: The HA hydrogel matrices were prepared as described earlier and kept for 3 h at room temperature. For the subcutaneous implantation, the lumbar region was shaved and surgically prepared with three washes of alcohol. Then hydrogel constructs of 0.2 mL volume, and containing either 4 µg of BMP-2 ($n = 6$) or hydrogel

alone (n = 6) were injected subcutaneously with a 21 G needle, at a minimal distance of 15 mm apart. Immediately after intervention animals were administrated subcutaneously with buprenorfin (Temgesic, Schering-Plough, Brussels, Belgium, 0.05 mg/kg) for pain mitigation. Rats were sacrificed after 7 weeks by CO_2 asphyxiation. The implants were dissected, extracted and analyzed by microcomputed tomography (micro CT). The samples were also retrieved for histological observation (n = 5 per group).

Histological Evaluation: Specimens were stored in 70% ethanol, completely decalcified using an electrophoresis system (Tissue-Tek Miles scientific, Histolab, Göteborg, Sweden) with formic acid, dehydrated, and embedded in paraffin wax. Serial cross sections were cut with a microtome to 5 µm, deparaffinized and stained. Representative slides were stained with hematoxylin/eosin (H&E, Merck), Masson's trichrome (Merck), and Sirius Red (Fluka). The histological sections were photographed on a bright field microscope (Eclipse TE 2000U, Nikon). For collagen observation, the histological sections were stained with 0.1% Sirius red dissolved in a saturated aqueous solution of picric acid (Fluka) for 1 h. The samples were rinsed with 0.5% acetic acid and the cross-sections were observed and photographed using polarized light microscopy with the slides inclined at 45° to the incident light.

Detection of Blood Vessels: The localization of newly formed blood vessels within the new bone area was determined by the proximity ligation assay (PLA). For this method, 5 µm cross-sections were treated with rat epithelial cells antibody (RECA-1, Abcam), deparaffinized at 45 °C for 20 h, dehydratated and placed in antigen retrieval solution (Dako) at 98 °C for 15 min. After 20 min cooling at room temperature the slides were rinsed with PBS and incubated in Tris-Buffered Saline (TBS: 500 mM Tris, 60 mM KCl and 2.8 M NaCl in high purity dH_2O, pH 7.4) for 2 min. The primary antibody anti-RECA-1 was diluted at 1:200 and incubated at 4 °C overnight. This was followed by the use of secondary probe ligation and amplification (Duolink II Kit) in accordance with manufactures protocol. The slides were coverslipped with Vectashield (Vector Laboratory) containing DAPI (100 ng/mL) and visualized in fluorescent microscopy (Eclipse TE 2000U, Nikon).

Supporting Information

Supporting Information is available from the Wiley Online Library or from the author.

Acknowledgements

The authors would like to thank Mr. Stefan Gunnarsson for his help with polarized light microscopy. This work has benefited from research funding from the European Community's Seventh Framework Programme in the project *Angioscaff* NMP-LA-2008–214402.

Received: June 22, 2012
Revised: September 17, 2012
Published online: October 12, 2012

[1] B. V. Slaughter, S. S. Khurshid, O. Z. Fisher, A. Khademhosseini, N. A. Peppas, *Adv. Mater.* **2009**, *21*, 3307–3329.
[2] M. P. Lutolf, J. A. Hubbell, *Nat. Biotechnol.* **2005**, *23*, 47–55.
[3] T. P. Kraehenbuehl, R. Langer, L. S. Ferreira, *Nat. Methods* **2011**, *8*, 731–736.
[4] O. P. Varghese, W. Sun, J. Hilborn, D. A. Ossipov, *J. Am. Chem. Soc.* **2009**, *131*, 8781–8783.
[5] K. Vulic, M. S. Shoichet, *J. Am. Chem. Soc.* **2012**, *134*, 882–885.
[6] D.-A. Wang, S. Varghese, B. Sharma, I. Strehin, S. Fermanian, J. Gorham, D. H. Fairbrother, B. Cascio, J. H. Elisseeff, *Nat. Mater.* **2007**, *6*, 385–392.
[7] N. A. Peppas, J. Z. Hilt, A. Khademhosseini, R. Langer, *Adv. Mater.* **2006**, *18*, 1345–1360.
[8] E. S. Place, N. D. Evans, M. M. Stevens, *Nat. Mater.* **2009**, *8*, 457–470.
[9] J. R. Watterson, J. M. Esdaile, *J. Am. Acad. Orthop. Surg.* **2000**, *8*, 277–284.
[10] H. J. Volker-Dieben, H. Regensburg, P. J. Kruit, *Cornea* **1994**, *13*, 414–417.
[11] J. A. P. Gomes, R. Amankwah, A. Powell-Richards, H. S. Dua, *Br. J. Ophthalmol.* **2004**, *88*, 821–825.
[12] N. J. Lowe, C. A. Maxwell, P. Lowe, M. G. Duick, K. Shah, *J. Am. Acad. Dermatol.* **2001**, *45*, 930–933.
[13] Y. Luo, K. R. Kirker, G. D. Prestwich, *J. Controlled Release* **2000**, *69*, 169–184.
[14] J. A. Burdick, G. D. Prestwich, *Adv. Mater.* **2011**, *23*, H41–H56.
[15] D. D. Allison, K. J. Grande-Allen, *Tissue Eng.* **2006**, *12*, 2131–2140.
[16] B. P. Toole, *Nat. Rev. Cancer* **2004**, *4*, 528–539.
[17] E. Martínez-Sanz, D. A. Ossipov, J. Hilborn, S. Larsson, K. B. Jonsson, O. P. Varghese, *J. Controlled Release* **2011**, *152*, 232–240.
[18] S. J. Bryant, K. S. Anseth, *J. Biomed. Mater. Res. A.* **2002**, *59*, 63–72.
[19] H. Park, X. Guo, J. S. Temenoff, Y. Tabata, A. I. Caplan, F. K. Kasper, A. G. Mikos, *Biomacromolecules* **2009**, *10*, 541–546.
[20] X. Huang, C. S. Brazel, *J. Controlled Release* **2001**, *73*, 121–136.
[21] R. Barbucci, S. Lamponi, A. Borzacchiello, L. Ambrosio, M. Fini, P. Torricelli, R. Giardino, *Biomaterials* **2002**, *23*, 4503–4513.
[22] P. Eiselt, K. Y. Lee, D. J. Mooney, *Macromolecules* **1999**, *32*, 5561–5566.
[23] J. A. Burdick, C. Chung, X. Jia, M. A. Randolph, R. Langer, *Biomacromolecules* **2005**, *6*, 386–391.
[24] W. S. Toh, T. C. Lim, M. Kurisawa, M. Spector, *Biomaterials* **2012**, *33*, 3835–3845.
[25] D. Y. Q. Wong, J. Y. Lau, W. H. Ang, *Dalton Trans.* **2012**, *41*, 6104–6111.
[26] J. Kalia, R. T. Raines, *Angew. Chem. Int. Ed.* **2008**, *47*, 7523–7526.
[27] A. R. Blanden, K. Mukherjee, O. Dilek, M. Loew, S. L. Bane, *Bioconjugate Chem.* **2011**, *22*, 1954–1961.
[28] O. P. Varghese, M. Kisiel, E. Martınez-Sanz, D. A. Ossipov, J. Hilborn, *Macromol. Rapid Commun.* **2010**, *31*, 1175–1180.
[29] J. P. A. Fairclough, A. I. Norman, *Annu. Rep. Prog. Chem., Sect. C: Phys. Chem.* **2003**, *99*, 243–276.
[30] S. Piskounova, R. Rojas, K. Bergman, J. Hilborn, *Macromol. Mater. Eng.* **2011**, *296*, 944–951.
[31] P. B. Welzel, S. Prokoph, A. Zieris, M. Grimmer, S. Zschoche, U. Freudenberg, C. Werner, *Polymers* **2011**, *3*, 602–620.
[32] M. Yoneda, M. Yamagata, S. Suzuki, K. Kimata, *J. Cell Science* **1988**, *90*, 265–273.
[33] J. N. Zara, R. K. Siu, X. Zhang, J. Shen, R. Ngo, M. Lee, W. Li, M. Chiang, J. Chung, J. Kwak, B. M. Wu, K. Ting, C. Soo, *Tissue Eng. Part A* **2011**, *17*, 1389–1388.
[34] S. Fredriksson, M. Gullberg, J. Jarvius, C. Olsson, K. Pietras, S. M. Gústafsdóttir, A. Östman, U. Landegren, *Nat. Biotechnol.* **2002**, *20*, 473–477.
[35] O. Soderöberg, K.-J. Leuchowius, M. Gullberg, M. Jarvius, I. Weibrecht, L.-G. Larsson, U. Landegren, *Methods* **2008**, *45*, 227–232.
[36] E. Buncel, I.-H. Um, *Tetrahedron* **2004**, *60*, 7801–7825.
[37] D. Dikovsky, H. Bianco-Peleda, D. Seliktar, *Biomaterials* **2006**, *27*, 1496–1506.
[38] E. J. Carragee, E. L. Hurwitz, B. K. Weiner, *Spine J.* **2011**, *11*, 471–491.
[39] U. Krause, S. Harris, A. Green, J. Ylostalo, S. Zeitouni, N. Lee, C. A. Gregory, *Proc. Natl. Acad. Sci. USA* **2010**, *107*, 4147–4152.
[40] J. Patterson, R. Siew, S. W. Herring, A. S. P. Lin, R. Guldberg, P. S. Stayton, *Biomaterials* **2010**, *31*, 6772–6781.
[41] M. Kerschnitzki, W. Wagermaier, P. Roschger, J. Seto, R. Shahar, G. N. Duda, S. Mundlos, P. Fratzl, *J. Struct. Biol.* **2011**, *173*, 303–311.